Int J Thermophys (2017) 38:72
DOI 10.1007/s10765-017-2215-9

ICPPP 18

# Analysis of the Measurement System and Optimization of the Measurement Procedure for Detection of Thermal Memory Effects by Photoacoustic Experiments

**S. Todosijević[1,2] · Z. Šoškić[2] · Z. Stojanović[3] · S. Galović[3]**

Received: 18 October 2015 / Accepted: 6 March 2017 / Published online: 17 March 2017


**Abstract** Experimental verification of thermal memory effects represents a challenge that is important from both fundamental and practical points of view. Recent theoretical studies suggest that the thermal memory effect should lead to thermal resonances in the modulation frequency characteristics of photoacoustic response. Therefore, studies of thermal resonances in photoacoustic response represent an alternative for detection of the thermal memory effect and measurement of thermal memory properties. Since the resonances were not observed, this paper analyzes standard measurement setups and shows that the experimental technique should be optimized to provide a better chance of detection of thermal memory effects by photoacoustic measurements. The results show that a proper selection of modulation frequencies and the knowledge of the approximate transfer function of the electronic part of the photoacoustic measurement system are prerequisites for detection of thermal resonances in the modulation frequency characteristics of photoacoustic response.

**Keywords** Photoacoustic effect · Thermal memory

This article is part of the selected papers presented at the 18th International Conference on Photoacoustic and Photothermal Phenomena.

✉ S. Todosijević
todosijevic.s@mfkv.kg.ac.rs

1 School of Electrical Engineering, University of Belgrade, Bulevar kralja Aleksandra 73, Belgrade, Serbia

2 Faculty of Mechanical and Civil Engineering, University of Kragujevac, Dositejeva 19, Kraljevo, Serbia

3 Vinča Institute of Nuclear Sciences, University of Belgrade, P. O. Box 522, Belgrade 11001, Serbia

## 1 Introduction

The classical Fourier theory of heat conduction describes the process by the constitutive equation $\vec{q} = -k \cdot \nabla T$ and the parabolic differential equation $\partial T/\partial t = D \cdot \nabla^2 T$, where $T$ stands for the temperature, $q$ for the heat flux, $t$ for the time, and $k$ and $D$ represent the thermal conductivity and the thermal diffusivity of the medium, respectively [1]. The approach treats heat propagation as a diffusion process, which means that the heat propagation speed is infinite, and thus, it contradicts the theory of relativity.

However, it has already been established that for the proper analysis of non-stationary heat propagation processes, such as heat pulse [2] and laser flash [3] experiments, it is necessary to treat the heat propagation process in a more general manner [4–6], which accounts for the finite speed of heat propagation. One of the simplest solutions for introducing a finite speed of heat propagation is the description of the heat propagation process by a hyperbolic equation $\tau \cdot \partial^2 T/\partial t^2 + \partial T/\partial t = D \cdot \nabla^2 T$, which requires the modified constitutive equation $\tau \cdot \partial \vec{q}/\partial t + \vec{q} = -k \cdot \nabla T$, with $\tau$ standing for the thermal relaxation time [7–11]. Such an approach treats heat propagation as a wave process with finite propagation speed, and the meaning of the constitutive equation is that the heat flux at one point depends on its values in the past. The dependence of the heat propagation process on its history is called *thermal memory*. Since the existence of thermal memory changes the nature of the heat propagation process, it has significant theoretical importance, but also practical consequences for the interpretation of non-stationary heat transfer phenomena and the characterization of thermal properties of matter.

The photoacoustic (PA) effect is the generation of sound waves in a sample and its surroundings due to the exposure to modulated optical radiation [12–19]. The effect was discovered and reported by A.G. Bell at the end of the nineteenth century, but the proper explanation was given almost one hundred years later [12]. The explanation and further theoretical studies were based on the classical heat propagation theory, and they boosted experimental research and practical applications of the PA effect, which confirmed the validity and applicability of theoretical models. However, due to the variable heat generation by modulated optical radiation, the PA effect causes an essentially non-stationary heat transfer process and recent theoretical studies [7–11,16–19] showed that thermal memory should affect PA response at sufficiently high modulation frequencies. The results of the theoretical studies predict the existence of thermal resonances in the modulation frequency characteristics of PA response, and resonant frequencies depend on the thermal relaxation time. The detection of thermal resonances in the modulation frequency characteristics of PA response, therefore, would not only confirm the existence of thermal memory but would also enable the calculation of thermal relaxation times of matter. However, with few insufficiently described exceptions [7,16–19], the thermal resonances in PA characteristics were not detected. Due to the potential importance, the absence of detection of thermal resonances in previous PA experiments requires due explanation. This paper analyzes various aspects of the experimental PA technique, with the aim to define the requirements that an experimental setup should meet in order to enable the detection of thermal resonances in the modulation frequency characteristics of PA response.

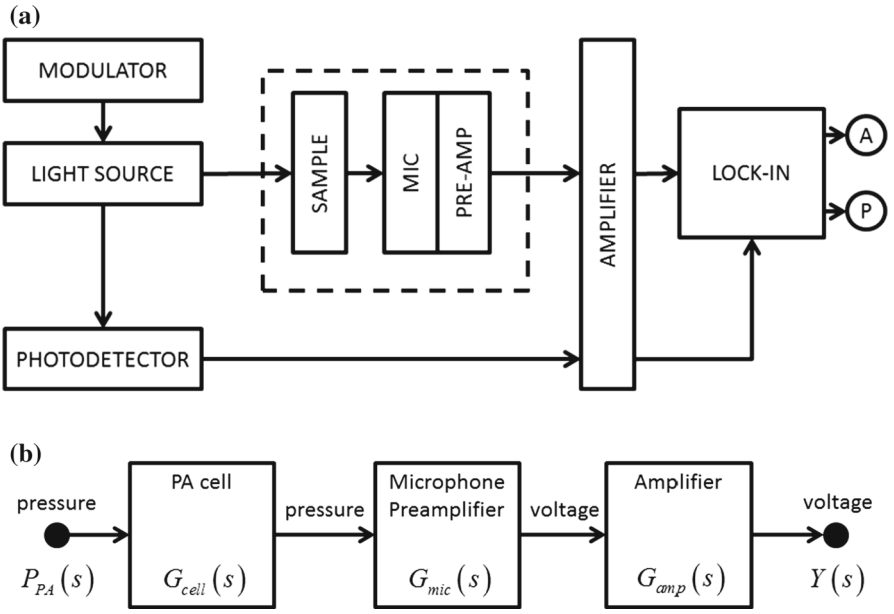


**Fig. 1** (a) Schematic representation of the photoacoustic measurement system; (b) block diagram of the photoacoustic measurement system

## 2 Theory

A conceptual diagram of the PA measurement system is presented in Fig. 1a. The light source emits light under control of the modulator. The modulator may use mechanical (such as a chopper with rotating blades) or electronic (control of the power supply of the light source) principles. Since the rotation speed of a modulator also has to be controlled, electronic modulation seems to be the preferable choice. Besides, electronic modulation allows simple implementation of various modulation forms. The modulated light beam irradiates the sample that absorbs a part of the light, and a part of the absorbed light is converted into heat.

Heat transfer through the sample causes deformation of the sample, and heat transfer to the surroundings causes expansion of the thin layer of the surrounding medium. The sound emission due to the deformation of the sample is called "direct" or "thermo-elastic" (TE) PA mechanism, and the sound emission due to the expansion of the surrounding medium is called "indirect" or "thermo-diffusion" (TD) PA mechanism. The relative contribution of the mechanisms to PA response depends on the geometric and material properties of the sample, as well as on the modulation frequency [20]. Within the framework of the classical Fourier heat conduction theory, the TD mechanism dominates at sufficiently low modulation frequencies, sufficiently thick samples, or samples with sufficiently low thermal expansion coefficients and thermal diffusivities, whereas the TE mechanism is dominant at sufficiently high modulation frequencies, sufficiently thin samples, or samples with sufficiently high thermal expansion coefficients and thermal diffusivities [20]. The relations that determine the relative

contributions of the mechanisms and the applicability of the respective approximations are given in [20]. However, if thermal memory is present, the frequency range where the TD component is dominant further increases [16,17].

The emitted sound waves propagate through a closed space of a PA cell and are detected by a microphone. The majority of microphones used in the PA experiments are audio microphones with the frequency range 20 Hz–20 kHz. If the microphone is placed at the irradiated side of the sample, then the experimental setup is called "the reflection PA configuration," and if the microphone is placed at the opposite side of the sample, the experimental setup is called "the transmission PA configuration." The signal of the microphone transducer is conditioned by the preamplifier of the microphone and led by a cable to an amplifier. The amplified microphone signal is led to one input of the lock-in detector. The amplified signal of the photodetector that is illuminated by the same optical beam as the sample is led to the other input of the lock-in detector. The output of the lock-in detector consists of two signals: (1) the ratio between the amplitudes of the signals of the microphone and the photodetector and (2) the phase difference between the signals.

The theoretical research on PA response that is based on the Fourier heat transfer theory [12–15,21–24] predicts that the amplitude of PA response monotonously decreases with an increase in modulation frequency. However, recent research [7–11,16–19] has shown that, due to thermal memory, the amplitude and the phase delay of PA response show the resonant behavior at sufficiently high frequencies. The resonant frequencies depend on the thermal properties and thickness of the sample, as well as on the thermal properties of the backing of the sample and the surrounding medium [16–19].

Paper [18] presents a detailed theory of the TD component of PA response in the media with thermal memory, and it has been shown that the limiting cases of the surrounding medium are the case when the backing of the sample is an ideal thermal insulator and the case when the backing of the sample is an ideal thermal conductor. For the case of a sample with the thickness $l$ and the ideal insulator backing in reflective configuration, the resonant maxima (denoted as ${\omega_{max\text{-}A\text{-}ins}}^{(m)}$) and minima (denoted as ${\omega_{min\text{-}A\text{-}ins}}^{(m)}$) of the amplitude are predicted at frequencies [18]

$$\omega^{(m)}_{max\text{-}A\text{-}ins} = 2m\frac{\pi}{2}\frac{u}{l}\cdot c\,(2m)\;\; \omega^{(m)}_{min\text{-}A\text{-}ins} = \frac{\pi}{2}\frac{u}{l}\cdot c\,(2m+1) \tag{1}$$

where $u$ is the speed of heat waves, given by $u = \sqrt{D/\tau}$, and $c(n)$ represents the factor $c(n) = (1 + (l/n \cdot \mu)^2)^{-1/2}$, where $\mu$ stands for the thermal diffusion length $\mu = 2\sqrt{D\tau}$. In the case of an ideal conducting backing, the positions of the minima and maxima are interchanged compared to the case with an ideal insulator backing [18]. The calculations of the factors $c(n)$ [18] show that for all practical purposes the resonant frequencies (1) may be considered equidistant.

The studies of the TE component of PA response in the media with thermal memory [19] predict a similar resonant behavior. The research has also shown [18,19] that the magnitude of resonances and resonant frequencies decreases with an increase in the thickness of the sample so that resonances are detectable only for thin samples, which satisfy the condition $l < \mu$.

## 3 Results and Discussion

The measurements of thermal relaxation times have not been performed by now. Theoretical estimations from various sources [7,9,18] report values in the range $10^{-14}$ s for superconductors to $10^{2}$ s for processed meat. Table 1 presents the estimations of heat wave speed $u$, the thermal diffusion length $\mu$ and minimum resonant frequencies for various materials, based on the theoretical estimations of the relaxation time and experimental measurements of diffusivity. The table shows that the minimum frequencies of thermal resonances are close to $1/\tau$, so that they belong to the audio-frequency range, which is used in PA experiments, only for some classes of soft matter (polymers, tissues, etc.), which explains the absence of thermal resonances in the majority of measured PA modulation frequency characteristics.

The presence of periodic thermal resonances could be considered confirmed if at least two resonances could be clearly distinguished in the recorded PA modulation frequency characteristics and if the resonant frequencies satisfy conditions given by (Eq. 1). It means that the modulation frequencies should be selected in a proper range and with proper resolution in order to detect the resonances with sufficient details to determine the positions of minima and maxima. From the equations given by (Eq. 1), it follows that, in order to detect $n$ resonances, the modulation frequency range should be $n$ times wider than the lowest thermal resonant frequency. Since the resonant frequencies are approximately equidistant, the modulation frequencies selected for recording of the modulation frequency characteristic should have a constant step ($f_{n+1} - f_n = f_n - f_{n-1}$) and not the proportional step ($f_{n+1}/f_n = f_n/f_{n-1}$), which is usual in acoustic experiments. The equations (Eq. 1) also show that, in order to record $n$ points belonging to a resonant peak, the frequency step of the modulation frequency should be $n$ times smaller than the respective resonant frequency.

In order to avoid confusion of thermal resonances with other resonant phenomena in the system, the resonant mechanisms in the PA cell should be studied to determine whether their resonant frequencies belong to the audio-frequency range. For the resonant mechanisms with resonant frequencies in the audio-frequency range, a data processing procedure that removes their influence on the recorded PA modulation frequency characteristics should be developed. Since a PA cell consists of a sample (as the sound emitter), an air column (as the sound transmitter), and a microphone (as the sound receiver), the resonant phenomena in the PA cell are resonances of the sample, resonances of the air column, and resonances of the microphone.

Mechanical resonances of the sample may be the resonances of longitudinal vibrations of the sample and the resonances of oscillations of the sample on the elastic supports. The frequency of the first harmonic of longitudinal vibrations of the sample $f_l$ may be calculated as $f_l = c_S/4l$, where $c_S$ stands for the speed of sound in the sample. If it is assumed that the minimum speed of sound in solids is higher than 1000 $\mathrm{m \cdot s^{-1}}$, and the length of the sample is in the sub-millimeter range, it can be concluded that the frequency of the first harmonic of longitudinal vibrations of the sample is close to the MHz range, far above the audio-frequency range. In the cases where the sample is supported by an elastic support (like rubber), the elastic constant of the support $k_{sup}$ may be estimated as $k_{sup} = E_{sup} \cdot S_{sup}/l_{sup}$ with $E_{sup}$, $S_{sup}$ and $l_{sup}$ standing for the Young modulus, the cross section and the length of the support.

**Table 1** Estimated order of the magnitude of the minimum resonant frequency in various classes of materials

| Material type | Thermal diffusivity ($m^2 \cdot s^{-1}$) | Thermal relaxation time (s) | Heat propagation speed ($m \cdot s^{-1}$) | Thermal diffusion length (m) | Minimum resonant frequency (Hz) |
|---|---|---|---|---|---|
| Low-order materials | | | | | |
| Metals | $10^{-5}-10^{-4}$ | $10^{-14}-10^{-12}$ | $10^{3}-10^{5}$ | $10^{-10}-10^{-8}$ | $10^{12}-10^{14}$ |
| Semiconductors | $10^{-6}-10^{-4}$ | $10^{-12}-10^{-8}$ | $10^{1}-10^{4}$ | $10^{-9}-10^{-6}$ | $10^{8}-10^{12}$ |
| High-order materials | | | | | |
| Alloys | $10^{-6}$ | $10^{-8}-10^{-6}$ | 1–10 | $10^{-7}-10^{-6}$ | $10^{6}-10^{8}$ |
| Doped semiconductors | $10^{-6}$ | $10^{-8}-10^{-6}$ | 1–10 | $10^{-7}-10^{-6}$ | $10^{6}-10^{8}$ |
| Polymers | $10^{-8}-10^{-7}$ | $10^{-8}-10^{-1}$ | $10^{-4}$–1 | $10^{-8}-10^{-4}$ | 10–$10^{8}$ |
| Tissues | $10^{-8}-10^{-7}$ | 1–100 | $10^{-5}-10^{-3}$ | $10^{-8}-10^{-2}$ | $10^{-2}$–10 |

With typical values for rubber supports, the elastic constant of the support has the order higher than $10^4\ \mathrm{N}\cdot\mathrm{m}^{-1}$. If the oscillations of the sample on the support may be considered as the oscillations of the spring-mass system, then its resonant frequency may be calculated as $f_{ss} = \sqrt{k_{sup}/m_s}$, and with typical masses of the sample $m_S$ of the order of milligram, the resonant frequency is of the order of 100 kHz, so also above the audio-frequency range.

The air column in the PA cell may have two kinds of mechanical resonances, resonant longitudinal vibrations of the air column and Helmholtz resonances. The resonant frequencies of vibrations of the air column may be estimated as the resonant frequencies of longitudinal vibrations of the air column closed on both sides along the axis of the PA cell. The frequency of the first harmonic of vibrations $f_A$ may be calculated as $f_A = c_A/2L_A$, where $c_A$ stands for the speed of sound in air and $L_A$ stands for the length of the air column in the PA cell. For usual configurations, measurements are performed at room temperature and atmospheric pressure, when the speed of sound is close to $340\ \mathrm{m}\cdot\mathrm{s}^{-1}$, and the length of the air column is few millimeters. It can be concluded that the frequency of the first harmonic of longitudinal vibrations of the air column is higher than 100 kHz so that the resonant frequencies are far above the audio-frequency range. The Helmholtz resonance of the open-ended PA cell has been studied in the paper [25]. The simplest estimation of the resonant frequency of a closed Helmholtz resonator is $f_H = c_A/2\pi\sqrt{S/Vl}$, with $V$ standing for the volume of the PA cell, and $S$ and $l$ standing for the cross section and the length of the inlet of the PA cell, respectively. With usual dimensions of the PA cell, the resonant frequency is close to 20 kHz and may belong to the audio-frequency range.

The resonant frequency of the microphone depends on the type of the microphone and its dimensions, with smaller microphones having higher resonant frequencies. The electret microphones that have high resonant frequencies of the order of several kHz [26] are predominantly used in PA measurements.

One of the methods for distinguishing thermal resonances from other resonances in PA measurements is decomposition of the transfer function of the measurement system. The processes in optical electronic components (light source and photodetector) are much faster than the processes in electronic and mechanic components of the PA measurement system, and the transfer functions of the optoelectronic components may be considered flat in the audio-frequency range. Since the bandwidth–gain product of the lock-in detectors is of the order of MHz and the input signals to the lock-in detector are already amplified, the transfer function of the lock-in detector may also be considered flat in the audio-frequency range. Therefore, the remaining part of the PA measurement system may be represented by the block diagram in Fig. 1b. Using the block diagram, the Laplace transform of the output of the amplifier $Y(s)$ may be represented as: $Y(s) = P_{PA}(s)G(s) = P_{PA}(s)G_{cell}(s)G_{mic}(s)G_{amp}(s)$, where $P_{PA}(s)$ stands for the Laplace transform of PA response of the sample, $G_{cell}(s)$ stands for the transfer function of propagation of pressure through the PA cell, $G_{mic}(s)$ stands for the transfer function of the microphone with the preamplifier and $G_{amp}(s)$ stands for the transfer function of the amplifier. If the transfer function of the PA measurement system $G(s)$ is known, then the amplitude $P_{\mathrm{PA}}(\omega)$ and the phase $\varphi_{\mathrm{PA}}(\omega)$ of PA response may be extracted from the PA measurement data as

$$P_{PA}(s) = \frac{Y(s)}{G(s)} \Rightarrow P_{PA}(f) = \frac{Y(f)}{|G(j2\pi f)|} \quad \varphi_{PA}(f) = \varphi_Y(f) - \arg G(j2\pi f) \tag{2}$$

where $Y(f)$ and $\varphi_Y(f)$ represent the amplitude and the phase outputs of the lock-in detector at the modulation frequency $f$.

The transfer function may be constructed using the data obtained in the calibration process, i.e., measurement of the output of a system that is exposed to a known input. Various calibration methods use different types of input signals. Acoustic systems are usually calibrated by harmonic input and white noise input. Calibration by harmonic input provides both amplitude and phase delays of the transfer function that is studied, but reconstruction of a complete transfer function requires numerous repetitions of measurements with different frequencies, which makes the reconstruction of the transfer function using harmonic input calibration a long process. On the other hand, calibration by white noise enables reconstruction of a complete transfer function $G(s)$ by a single measurement. The procedure implies replacement of the sample in the PA cell by a white noise source and measurement of the output of the amplifier. The amplitude–frequency spectrum of the recorded output of the amplifier represents the amplitude of the transfer function $G(s)$. However, since the phase spectrum of white noise is usually not known, the phase delay of the transfer function $G(s)$ cannot be determined by the described procedure. Although there are other white noise calibration procedures, which use the phase of white noise, they are more complex and slow, so that the described procedure of measurement of the amplitude of the transfer function $G(s)$ may be complemented by reconstruction of the complete transfer function using an approximate transfer function of a model of the PA measurement system. The approximate transfer function is constructed as the product of approximate transfer functions of the PA cell, the microphone, and the amplifier, as it will be described in the following text.

Since the dimensions of the PA cell are much smaller than the wavelengths of sound in the audio-frequency range, and the frequencies of vibration resonances of the air column in the PA cell are well above the audio-frequency range, the transfer function of the PA cell may be considered constant in the audio-frequency range, except when the Helmholtz resonance frequency affects the transfer function in the audio-frequency range. The existence of one resonant frequency suggests that the transfer function of the PA cell in the audio-frequency range may be written as the transfer function of a second-order system [27],

$$G_{cell}(s) = \frac{\omega_H^2}{s^2 + 2\zeta_H \omega_H s + \omega_H^2} \tag{3}$$

with $\omega_\mathrm{H}$ and $\zeta_\mathrm{H}$ being the resonant frequency and the attenuation of the Helmholtz resonance [18].

A typical amplitude–frequency characteristic of a microphone is presented in Fig 2a. The important features of the characteristic are the high-frequency filtering at low frequencies and the resonant frequency at high frequencies. The microphone resonances at high frequencies have already been discussed. The high-frequency filtering is caused by the openings in the microphone membrane that provide balancing of static

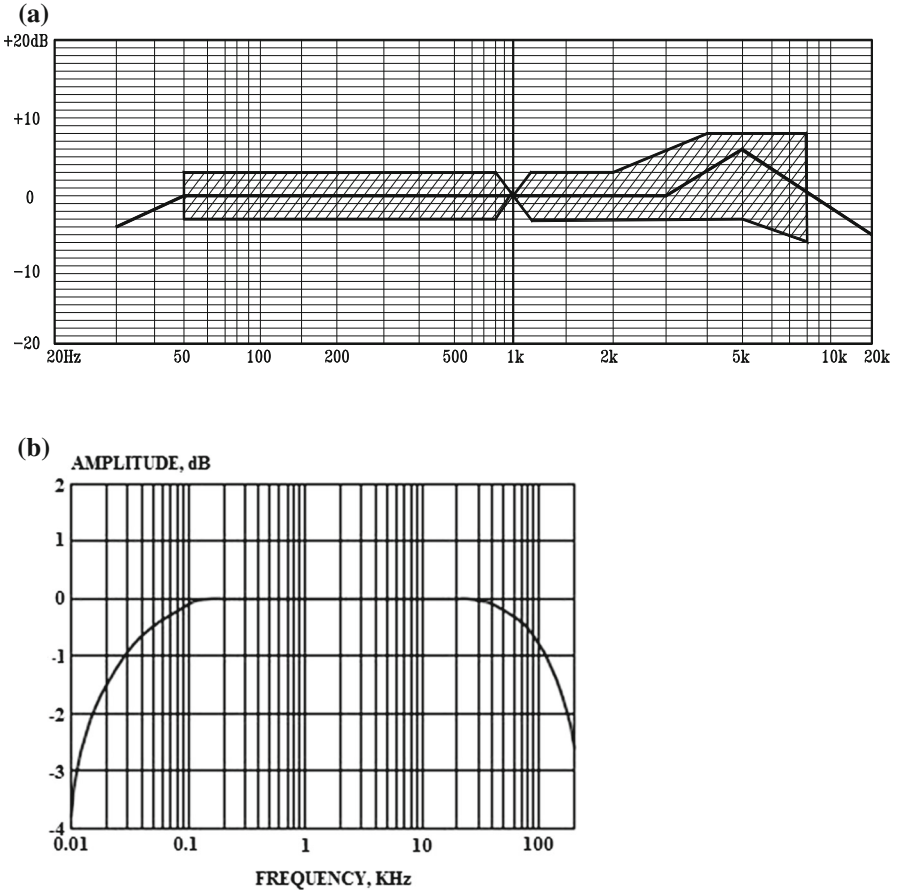


**Fig. 2** (a) Typical frequency response of an electret microphone and (b) typical frequency response of an audio amplifier

air pressure from both sides of the membrane. The openings prevent deformations of the membrane due to the variations of atmospheric pressure, but at the same time, they attenuate the response to low-frequency pressure changes, effectively acting as a high-frequency filter with a low cutoff frequency. Therefore, the approximate transfer function of the microphone may be given as the product of the transfer function of a high-frequency filter and a second-order system that has the resonant frequency of the microphone [27],

$$G_{mic}(s) = \frac{s}{s+\omega_{m1}} \frac{\omega_{m2}^2}{s^2 + 2\zeta_{m2}\omega_{m2}s + \omega_{m2}^2} \tag{4}$$

with $\omega_{m1}$ standing for the cutoff frequency of the high-frequency filter, and $\omega_{m2}$ and $\zeta_{m2}$ being the resonant frequency and the attenuation of the microphone resonance.

A typical amplitude–frequency characteristic of an audio amplifier is given in Fig. 2b. The important features of the characteristic are high-frequency filtering at low frequencies and low-frequency filtering at high frequencies. The high-frequency filtering at low frequencies is the consequence of the input capacitor that removes the DC component of the input signal before amplification. Similar to the case of the microphone, the capacitor and the input resistance of the amplifier represent a high-frequency filter. However, the values of the input capacitor and the resistance are sufficiently high that the cutoff frequency of the high-frequency filter is far below the audio-frequency range. The bandwidth of audio amplifiers is inversely proportional to their gain so that the bandwidth–gain product is the constant of an audio amplifier. Therefore, the low-frequency filter has the cutoff frequency approximately $B/A$, where $B$ stands for the bandwidth and $A$ stands for the gain of the amplifier. Consequently, the transfer function of an amplifier may be approximated in the audio-frequency range as the transfer function of the high-frequency filter with the cutoff frequency $B/A$ [27]:

$$G_{amp}(s) = \frac{2\pi \cdot B/A}{s + 2\pi \cdot B/A} \tag{5}$$

Therefore, the transfer function of the PA measurement system may be approximated in the audio-frequency range with the expression

$$G(s) = K \frac{s}{s + \omega_{m1}} \cdot \frac{2\pi \cdot B/A}{s + 2\pi \cdot B/A} \cdot \frac{\omega_{m2}^2}{s^2 + 2\zeta_{m2}\omega_{m2}s + \omega_{m2}^2} \cdot \frac{\omega_H^2}{s^2 + 2\zeta_H\omega_H s + \omega_H^2} \tag{6}$$

The parameters of the transfer function $\omega_{m1}$, $\omega_{m2}$, $\zeta_{m2}$, $\omega_H$, $\zeta_H$, $A$ and $B$ should be determined by plotting the log–log diagram of the spectrum of the response of the PA measurement system to white noise and recognizing the characteristic features in the obtained plot. If some of the features are missing, then the corresponding characteristic frequency should be considered infinite. Once the approximate transfer function in the form (Eq. 6) is known, the equations (Eq. 2) may be applied to determine PA response.

## 4 Conclusion

The paper presented an analysis of the photoacoustic measurement setup and procedure that should reveal why thermal memory effects are not detected in the modulation frequency characteristics of PA response, despite theoretical predictions. The analysis also provided some instructions for future PA experiments that intend to detect the predicted thermal resonances in the modulation frequency characteristics of PA response and provide support to the theory of thermal memory of matter.

The results of the analysis have shown that the values of the lowest resonant frequencies that may be detected in a material are close to the inverse thermal relaxation time of the material. Therefore, thermal resonances are expected in the modulation frequency range of usual PA experiments only for thin samples with thermal relaxation times longer than a millisecond, which means only for soft matter samples with

sub-millimeter thickness. Since detection of a single resonance would not confirm the predicted thermal memory effects, multiple resonances should be detected, which means that the frequency of the first harmonic of thermal resonances should be several times smaller than the modulation frequency range. The analysis has also shown that the modulation frequency step in measurements should be constant, and not proportional because thermal resonant frequencies are approximately equidistant. The modulation frequency step should be at least an order of magnitude smaller than the resonant frequency to provide sufficient resolution to the detected resonant peaks.

Furthermore, the resonances detected in the modulation frequency characteristics have to be separated into the resonances of the measurement system and thermal resonances. The presented analysis considers mechanical resonances of the sample, the air column in the PA cell, and the microphone. The results of the analysis have shown that the resonance of the microphone and the Helmholtz resonance in the case of transmission configuration have resonance frequencies in the audio-frequency range, so that they may be confused with thermal resonances in PA experiments. The paper presents an approximate model of the PA measurement system, which enables separation of thermal resonances from other resonances that arise in the system.

**Acknowledgements** This work was funded by the Ministry of Education, Science and Technological Development of the Republic of Serbia through research Projects TR-37020 and III 45005.

## References

1. H.S. Carslaw, J.C. Jaeger, *Conduction of Heat in Solids*, 2nd edn. (Clarendon Press, Oxford, 1959)
2. W. Dreyer, H. Struchtrup, Heat pulse experiments revisited. Contin. Mech. Thermodyn. **5**, 3–50 (1993)
3. T. Baba, N. Taketoshi, T. Yagi, Development of ultrafast laser flash methods for measuring thermophysical properties of thin films and boundary thermal resistances. Jpn. J. Appl. Phys **50**, 11RA01 (2011)
4. P. Ván, B. Czél, T. Fülöp, G. Gróf, Á. G. J. Verhás, Experimental aspects of heat conduction beyond Fourier (2013), arXiv:1305.3583
5. R. Kovács, P. Ván, Generalized heat conduction in heat pulse experiments. Int. J. Heat Mass Transf. **83**, 613–620 (2015)
6. P. Ván, Theories and heat pulse experiments of non-Fourier heat conduction (2015), arXiv:1501.04234
7. S. Galović, D. Kostoski, Photothermal wave propagation in media with thermal memory. J. Appl. Phys. **93**, 3063–3070 (2003)
8. D. Jou, J. Casas-Vázquez, G. Lebon, Extended irreversible thermodynamics. Rep. Prog. Phys. **51**, 1105 (1988)
9. K. Mitra, S. Kumar, A. Vedevarz, M.K. Moallemi, Experimental evidence of hyperbolic heat conduction in processed meat. J. Heat Transf. **117**, 568–573 (1995)
10. I.A. Novikov, Harmonic thermal waves in materials with thermal memory. J. Appl. Phys. **81**, 1067–1072 (1997)
11. S. Galović, Thermal effects induced by laser irradiation of solids, in *The Physics of Ionized Gases: 22nd Summer School and International Symposium on the Physics of Ionized Gases, Invited Lectures, Topical Invited Lectures and Progress Reports*, vol 740, No. 1, (AIP Publishing, 2004) pp. 221–232
12. A. Rosencwaig, A. Gersho, Theory of the photoacoustic effect with solids. J. Acoust. Soc. Am. **58**, S52–S52 (1975)
13. A.C. Tam, Applications of photoacoustic sensing techniques. Rev. Mod. Phys. **58**, 381 (1986)
14. H.K. Park, C.P. Grigoropoulos, A.C. Tam, Optical measurements of thermal diffusivity of a material. Int. J. Thermophys. **16**, 973–995 (1995)
15. G. Rousset, F. Lepoutre, L. Bertrand, Influence of thermoelastic bending on photoacoustic experiments related to measurements of thermal diffusivity of metals. J. Appl. Phys. **54**, 2383–2391 (1983)

16. D.D. Markushev, M.D. Rabasović, M. Nesic, M. Popovic, S. Galovic, Influence of thermal memory on thermal piston model of photoacoustic response. Int. J. Thermophys. **33**, 2210–2216 (2012)
17. M. Nešić, P. Gusavac, M. Popović, Z. Šoškić, S. Galović, Thermal memory influence on the thermo-conducting component of indirect photoacoustic response. Phys. Scr. **2012**, 014018 (2012)
18. S. Galović, Z. Šoškić, M. Popović, D. Čevizović, Z. Stojanović, Theory of photoacoustic effect in media with thermal memory. J. Appl. Phys. **116**, 024901 (2014)
19. M. Nesic, S. Galovic, Z. Soskic, M. Popovic, D.M. Todorovic, Photothermal thermoelastic bending for media with thermal memory. Int. J. Thermophys. **33**, 2203–2209 (2012)
20. Z. Šoškić, S. Ćirić-Kostić, S. Galović, An extension to the methodology for characterization of thermal properties of thin solid samples by photoacoustic techniques. Int. J. Therm. Sci. **109**, 217–230 (2016)
21. J.A. Balderas-Lopez, A. Mandelis, Self-normalized photothermal technique for accurate thermal diffusivity measurements in thin metal layers. Rev. Sci. Instrum. **74**, 5219–5225 (2003)
22. J.A. Balderas-Lopez, Self-normalized photoacoustic technique for thermal diffusivity measurements of transparent materials. Rev. Sci. Instrum. **79**, 024901 (2008)
23. D.D. Markushev, J. Ordonez-Miranda, M.D. Rabasović, S. Galović, D.M. Todorović, S.E. Bialkowski, Effect of the absorption coefficient of aluminium plates on their thermoelastic bending in photoacoustic experiments. J. Appl. Phys. **117**, 245309 (2015)
24. J.L. Pichardo, E. Marin, J.J. Alvarado-Gil, J.G. Mendoza-Alvarez, A. Cruz-Orea, I. Delgadillo, G. Torres-Delgado, H. Vargas, Photoacoustic measurements of the thermal properties of AlyGa1-yAs alloys in the region $0 < y < 0.5$. Appl. Phys. A **65**, 69–72 (1997)
25. M.N. Popovic, M.V. Nesic, S. Ciric-Kostic, M. Zivanov, D.D. Markushev, M.D. Rabasovic, S.P. Galovic, Helmholtz resonances in photoacoustic experiment with laser-sintered polyamide including thermal memory of samples. Int. J. Thermophys. **37**, 116 (2016)
26. B. Goelzer, C.H. Hansen, G. Sehrndt, *Occupational Exposure to Noise: Evaluation, Prevention and Control* (World Health Organisation, Geneva, 2001)
27. K. Ogata, *Modern Control Engineering*, 5th edn. (Prentice Hall, Upper Saddle River, 2010)